ELSEVIER

Seminars in
RADIATION
ONCOLOGY

Deformable Registration for Dose Accumulation

Indrin J. Chetty, PhD,* and Mihaela Rosu-Bubulac, PhD†

As deformable image registration makes its way into the clinical routine, the summation of doses from fractionated treatment regimens to evaluate cumulative doses to targets and healthy tissues is also becoming a frequently utilized tool in the context of image-guided adaptive radiotherapy. Accounting for daily geometric changes using deformable image registration and dose accumulation potentially enables a better understanding of dose-volume-effect relationships, with the goal of translation of this knowledge to personalization of treatment, to further enhance treatment outcomes. Treatment adaptation involving image deformation requires patient-specific quality assurance of the image registration and dose accumulation processes, to ensure that uncertainties in the 3D dose distributions are identified and appreciated from a clinical relevance perspective. While much research has been devoted to identifying and managing the uncertainties associated with deformable image registration and dose accumulation approaches, there are still many unanswered questions. Here, we provide a review of current deformable image registration and dose accumulation techniques, and related clinical application. We also discuss salient issues that need to be deliberated when applying deformable algorithms for dose mapping and accumulation in the context of adaptive radiotherapy and response assessment.
Semin Radiat Oncol 29:198–208

Introduction

The utilization of imaging in radiation oncology is indeed ubiquitous. Imaging is required for cancer staging, target and normal volume definitions for treatment planning, accurate localization for targeting prior to and during radiation delivery, and response assessment during and after the course of radiation therapy. Although CT-based imaging has served as the "work horse" modality, the integration of multimodal methods for both geometric and functional imaging, such as PET, MRI, ultrasound, optical approaches, and other techniques, forms a pivotal component of the overall imaging suite required for accurate, and individualized staging, treatment planning and delivery, and follow-up of cancer patients treated with radiation therapy.[1-4] The success of the extraction of relevant and accurate information from acquired images is entirely dependent on the image processing approaches and algorithms used for specific purposes.[5] In particular, image registration, in which 2 or more images are registered to a common coordinate system, is an essential process for manipulation of images in radiation therapy. Image registration enables extraction of geometric and/or functional information from images for a variety of purposes, such as creation of patient models in simulation and planning, localization and monitoring of patient anatomy during treatment, and assessment of tumor and normal organ response during and postradiation therapy.

The goal of an image registration technique is to find the transformation that optimally aligns corresponding points or structures in the 2 image datasets. Generally speaking, image registration algorithms have been classified according to "rigid" approaches, where the registration transformation only requires translation and/or rotation to bring into alignment corresponding points, or "non-rigid" or "deformable," where due to shape changes or distortion between structures in the 2 image datasets, stretching of the image grid to morph the corresponding points into alignment is required by the transformation. Exhaustive reviews of the fundamentals of image registration and associated rigid and deformable algorithms are provided elsewhere.[4,6-11]

This article covers the application of deformable image registration (DIR) algorithms for the purposes of dose accumulation, or deformable dose accumulation. The accuracy of deformable dose mapping and accumulation is entirely

*Department of Radiation Oncology, Henry Ford Cancer Institute, Henry Ford Health System, Detroit, MI
†Department of Radiation Oncology, Virginia Commonwealth University, Richmond, VA
Conflict of Interest: None.
Address reprint requests to Indrin J. Chetty, Department of Radiation Oncology, Henry Ford Cancer Institute, Henry Ford Health System, 2799 W. Grand Boulevard, Detroit, MI 48202. E-mail: lCHETTY1@hfhs.org

https://doi.org/10.1016/j.semradonc.2019.02.002
1053-4296/

dependent on the integrity of the underlying displacement vector field (DVF) generated during deformable image registration. Errors and uncertainties in the DVF will propagate directly to the dose mapping process. Therefore, salient aspects of deformable registration will be discussed before examining the directly linked concepts of dose mapping and dose accumulation, contemporary methods for accumulating dose, and associated challenges.

Deformable Image Registration: Fundamentals

Informative reviews on the image registration process and DIR algorithms are provided by Kessler[8] and others.[4,6-14] Here, we present the basics. The process of registering source and target image datasets can generally be broken down in the following 3 basic components: (1) the transformation model which is the mathematic model describing the manner in which the source image is warped to match the target image; (2) the similarity metric, which is the measure of how well the source (also noted primary, reference, or fixed) and target (also noted secondary or moving) image datasets match; and (3) the strategy used to optimize the transformation model parameters such that the source and target are aligned based on the specified similarity metric.

Transformation Models

The transformation model defines the type of deformation performed to bring source and target image datasets into alignment. The output of the transformation model, which produces the optimal mapping between features in source and target images, is commonly termed the displacement or DVF. There are numerous deformable transformation models ranging in complexity from those defined by a relatively small number of parameters modeling smooth regional variation, to completely relatively few parameters, to "free form" models in which each voxel in the volume can move independently, represented by a much larger number of parameters.[7,8,11] Spline-based algorithms are a commonly used deformation transformation model in which corresponding control points or "knots" are used in the source and target images, and spline functions are defined to model correspondences away from these points. B-spline-based transformations have become quite popular in the field of deformable image registration as they are found to be robust over a variety of anatomic sites, and are generally computationally efficient. Other transformation approaches include elastic, fluid and optical flow, and finite element models, which employ "free-form" or nonparametric transformations, where displacements for the individual voxel displacements are solved by local driving forces. Details about these types of models can be found elsewhere.[11]

Similarity Metrics

The level of agreement (or disagreement) of the registration process is measured by the similarity metric.[7,8,11,12] These metrics are typically divided into geometric and intensity-based approaches. Geometric approaches involve defining correspondences between source and target images based on anatomical elements defined in the images. These elements can include anatomical landmark points or implanted fiducial markers, as well as curves or surfaces. The typical registration metric looks to minimize the sum of squared differences between homologous (corresponding) points. Limitations of geometric-based approaches include the fact that alignment of geometric structures ignores anatomical distortions that may occur in other areas of the image outside these structures.[8] Intensity-based similarity measures align intensity patterns (gray-scale information) between source and target images based on specified mathematical criteria. Measures of intensity similarity are defined between image datasets and the transformation adjusted until the similarity measure is optimized. Clinically used similarity metrics include sum of squared intensity differences, cross correlation, and mutual information (MI). MI is a common metric which provides a measure of the intensity similarity between source and target images — it is assumed that the images will be most similar when they are most accurately registered at which point the mutual information between the images is maximized.[8]

Optimization Strategies

The optimization strategy refers to the mathematical approach used to adjust the transformation to optimize the similarity metric. Analogous to intensity modulated radiation therapy (IMRT) optimization in radiation treatment planning,[8] the registration optimizer works to find the best tradeoff among the competing demands related to finding the best correspondences subject to the specific type of application. In general, the type of optimization strategy best suitable for a specific application depends on several factors, including the cost function, transformation, accuracy requirements, and possible time constraints.

Task-Specific Constraints

As described by Sotiras et al,[11] deformable image registration is an ill-posed problem since the number of parameters to be determined in the transformation is superior to the constraints/information provided by the data. Regularization, the process of introducing additional information, such as prior knowledge of the underlying anatomical structure, is necessary to solve this ill-posed problem, and can help prevent local minima traps in the optimization. Regularization schemes include the use of penalization terms for nonphysical deformations, as well as constraints, such as topology preservation, volume preservation, and rigidity constraints (eg, for organs such as bones to prevent warping of such rigid structures). Other useful constraints imposed on the transformation model include inverse consistency and symmetry[11,15-20] — the mapping from source-to-target (forward transformation) and from target-to-source (forward transformation) are inverse mappings of each other.[11] Proper regularization and task-specific constraints can often be helpful toward generating DVFs that are less impaired by nonphysical (eg, unrealistic

compression or stretching of structures, voids in the mapping, etc.) deformations.

Validation of Deformable Image Registration

Evaluation of the overall registration process with the goal of ensuring accurate and consistent image registration, also referred to as validation, is necessary prior to clinical application. Uncertainties and errors in the registration transformation not only impact the quality of the alignment of structures or contours, but are also directly correlated to the mapped dose distributions. Therefore, it is essential to evaluate accuracy of the registrations, and identify regions where the registration is prone to higher and potentially clinically relevant uncertainties. A fundamental challenge with regard to validation for deformable alignment of arbitrary clinical image sets is that the ground truth is not known. In fact, given the ill-posed nature of the registration problem the true point-to-point correspondences may not even exist.[7] Consequently, comprehensive qualitative and quantitative approaches for assessment of registration accuracy have been developed, as detailed in the AAPM Task Group report No. 132, and other publications.[6-10,12,21] In general, recommended requirements for deformable registration algorithms at the planning stage are such that relevant boundaries and features of anatomy in the registered images are within 1-2 voxels of the registered image, and that additional sources of error be folded into the planning margins.[6]

Deformable Dose Mapping and Accumulation

Historically, the dose accumulation tool emerged in conjunction with treatment planning in the presence of breathing motion, to account for the changes in anatomy prompted by respiration (tumor movement, organ at risk (OAR) location, and/or volume changes) and the subsequently induced dose perturbations, with the ultimate goal of describing more accurately the planned dose for the time-varying anatomy. In this context, the dose accumulation is the process by which individual doses generated on datasets describing the anatomy at various respiratory phases are combined to create a composite dose. Differently put, accumulating doses adds a temporal dimension to the conventional 3D dose. Inconsistencies in patient anatomy are not only due to variations from the breathing pattern exhibited at the time of simulation but also due to other changes, often less predictable, such as weight loss and tumor shrinkage or growth. In addition, patient retreatments are often required, at times, years apart, and properly accounting for prior doses is necessary in order to prevent damaging overexposure to organs at risk. Approximate paradigms have been long employed to estimate doses to critical organs in such situations, but the obvious downside is that curative doses may sometimes be out of reach due to the overestimation of the dose to the uninvolved tissues.

With the above scenarios in mind, dose accumulation is, in the most general sense, a composite dose where the component doses are generated on 3D anatomical models acquired at different points in time, with the time scale ranging from seconds to years. Ideally, the "accumulation" would add doses on a "per anatomical unit" basis; if that were feasible, one would aim at tracking the dose in each body cell from one anatomical instance to another. However, with the anatomy digitized by a mere computer, the voxels that make up the dose matrix in the reference 3D image dataset are the proxies fulfilling the role of the tissue elements tracked over time. The tool used to morph one anatomy into another is the image registration, which establishes the one-on-one correspondence between the homologous entities from the anatomies considered. More specifically, the *deformable* image registration is the keystone in computing cumulative doses, because the patient's anatomy changes nonrigidly over any time scale (anyways, if changes were rigid, presumably they could be corrected solely through patient alignment). The transformation provided by the image registration, describing how a secondary anatomy changed compared to the reference anatomy, is u`sed to transfer the computed dose matrix from the secondary anatomy onto the reference anatomy. The process can be replicated with any number of secondary anatomies, after which, all the doses transferred to the reference anatomy can be summed to find the accumulated dose.

Formally, this can be expressed as in Eq. (1), for a series of M images ($J = \overline{1, M}$), of which R is the reference image:

$$D_{\text{accum}}(i) = D_R(i) + \sum_{J=1, J\neq R}^{J=M} D_J(i) = D_R(i) + \sum_{J=1, J\neq R}^{J=M} D_J\left(DVF_{JR}(i)\right) \quad (1)$$

where $D_{\text{accum}}(i)$ is the accumulated dose to a location i in the reference dataset R, $D_J(i)$ is the dose from secondary dataset J that is mapped onto i in the dataset R, $DVF_{JR}(i)$ is the DVF that describes which location from the secondary dataset J correlates with location i from the reference dataset R. How the "units" tracked are defined is typically a matter of convenience, and most often they are chosen to be the same as the *dose* grid voxels from the reference dataset, even though the DVF might have been defined for each *image* voxel (see Fig. 1).

The concept of dose accumulation is quite intuitive. However, the discrete (voxelized) nature of the data creates computational complications in mapping doses onto the reference dataset. The voxels in the secondary dataset are represented by a unique location – for example, their center of mass (COM); the COM can land, via image registration, anywhere inside a dose grid voxel from the secondary dataset, sometimes even together with other voxel centers from the reference image set. The next paragraphs will provide a historical review of how the dose mapping and the evaluation of the error in dose mapping evolved over time.

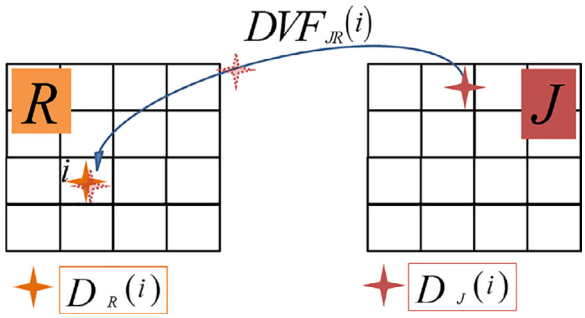

Figure 1 2D illustration of the dose accumulation. Location i in the reference dataset R receives a dose $D_J(i)$ from its homologous point in dataset, J in addition to the dose $D_R(i)$. $DVF_{JR}(i)$ describes the location where the point i from R is mapped onto J.

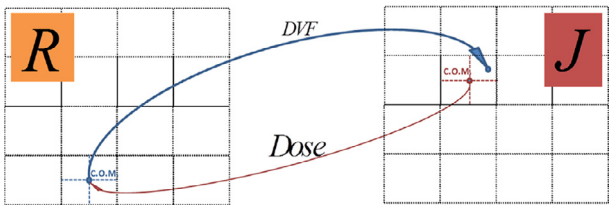

Figure 2 The principle of center-of-mass method for dose accumulation.

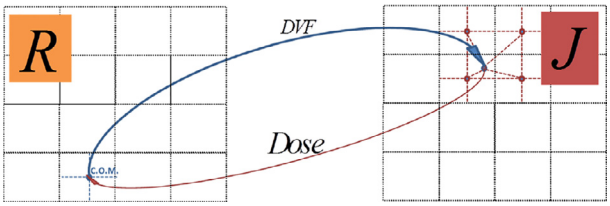

Figure 3 The principle of trilinear interpolation method for dose accumulation.

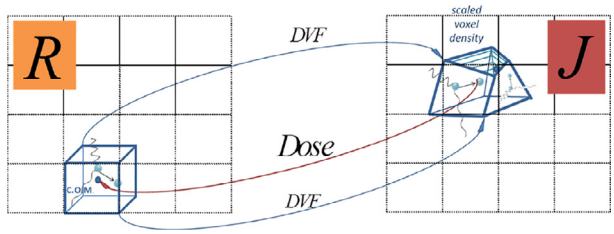

Figure 4 The principle of direct voxel tracking method for dose accumulation.

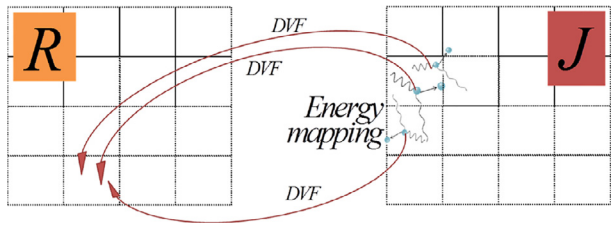

Figure 5 The principle of energy transfer method for dose accumulation.

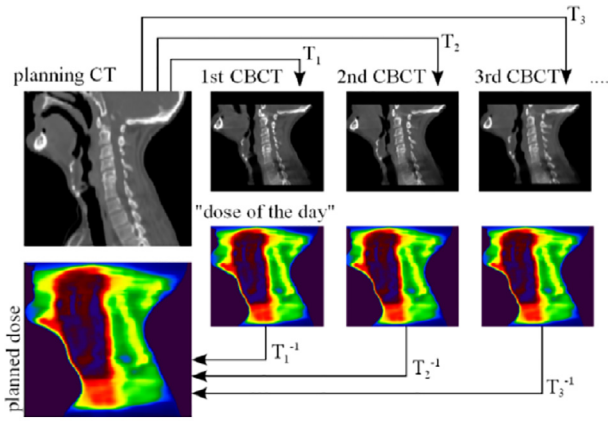

Figure 6 Example ART workflow, in which registration maps intensities from the CT to the daily CBCT scans, with the deformed or resampled CT used for "dose of the day" calculations. "Delivered dose" is mapped back to the planning stage, where it is accumulated. Adapted from Veiga et al.[46]

Dose Accumulation Methods

COM Method

The COM method is the most direct way to calculate the dose that a voxel from the reference dataset will receive from the dose grid computed on the secondary anatomy. The DVF provided by the image registration calculates the coordinates of each reference dose voxel COM when mapped on the secondary dataset; the dose voxel in which the mapped point lands is identified, and the reference dose voxel will then be assigned the dose from this voxel (which was scored at the COM of the secondary dataset dose voxel). In this approach, voxel shape/volume changes from one image set to another are not explicitly addressed (see Fig. 2).

The COM method was implemented in the Geant4 Monte Carlo code and demonstrated for a proton lung cancer irradiation case by Paganetti et al[22]; however, the approach can be used with any dose calculation algorithm, since the only quantity relevant to the problem is the dose per voxel in both the reference and the secondary dataset, scored at the voxel COM, regardless of the algorithm used to compute it.

Interpolation Methods

If the correlation between the reference and the secondary datasets is described by a nonrigid transformation, it is all but certain that a majority of the transformed reference voxels will not match any voxel from the secondary dataset in shape and/or volume. The dose to the mapped COM location in the secondary dataset can be approximated by using trilinear interpolation of the doses to the neighboring voxels of the mapped COM.[23-25] If larger local deformations are present, a finer trilinear interpolation can be used[23]: each voxel from the reference dataset is first subdivided into

octants, the center of each octant is mapped to locations on the secondary dataset dose grid, doses at tracked locations are estimated by trilinear interpolation, and their average value is scored back at the original dose grid center on the reference dataset (see Fig. 3).

The differences in the doses mapped on the reference datasets due solely to the interpolation method used did not seem to result in clinically significant changes in the relevant treatment plan metrics in the lung cases reviewed by Rosu et al, even though larger point dose differences were noted in high gradient regions, especially for larger dose grid sizes. As noted by Rosu et al,[23] the use of the refined interpolation is not necessarily equivalent to the use of the direct method at a finer grid resolution because the larger dose calculation grid inherits erroneous voxel dose estimation in the first place.

The major advantage of the interpolation methods is that they are fast; the disadvantage, at least in principle, is that the accuracy is degraded in regions of steep dose gradients. In addition to these geometric considerations, interpolation methods ignore the physical aspects of dose deposition as energy per mass. Also noteworthy is the fact that interpolation-based methods can be used with any dose computation engine.

Direct Voxel Tracking Method

Heath et al[26] proposed a direct voxel tracking method, implemented with a modified version of the DOSXYZnrc Monte Carlo dose code. Due to deformations, the rectangular voxels from the reference dataset become of an arbitrary shape on the secondary dataset (see Fig. 4). The particle transport in the secondary dataset is performed inside these deformed voxels, and the densities of the deformed voxels are adjusted to ensure mass conservation; thus, the energy deposited in a given mass of tissue is computed. The study reported a range of discrepancies between the voxel tracking and the trilinear interpolation method, with larger differences in the regions of steep dose gradients, at the entrance and distal surfaces of the study phantom, and for large voxel sizes (1 cm). Heath et al[26] also found that inaccuracies in the DVF cause, on average, 2% differences between the mass density in the secondary image and the density scaled from the reference dataset.

The initial implementation of this method was computationally expensive as a consequence of each "face" of the deformed voxel being approximated with 2 planes, forming dodecahedrons (the number of distance-to-voxel boundaries that need to be verified is doubled and additional testing is necessary to ensure that the particle-plane intersections occur inside the deformed voxel boundary). In a subsequent implementation,[27] each deformed voxel was divided in 6 tetrahedrons for dose transport, which roughly only doubled the computation time from the standard DOSXYZnrc.

Energy Transfer Methods

In an effort to reduce the computational resources required in the direct voxel tracking method, Siebers and Zhong[28] implemented an energy transfer method, where the energy deposition events in the secondary dataset are first simulated in a standard rectangular grid (thus removing the computational hardship of transporting particle within irregular boundaries), and then mapped onto the reference image. The dose to a voxel from the reference dataset was computed as the energy from the secondary dataset mapped to that reference voxel, divided by the mass of the voxel in the reference image (see Fig. 5). The method was further developed such that the mass mapping and the dose deposition mapping were performed using a consistent transformation between the datasets of interest: the energy from each dose deposition event on the secondary image is mapped onto the reference dataset and the warped mass of each reference voxel is computed from the secondary voxels using an equispace mapping approach (energy and mass congruent mapping energy mass congruence method (EMCM)).[29]

The energy transfer methods use the registration transformation that maps voxels from the secondary dataset onto the primary one, whereas the previously described methods use the mapping of voxels.

Li et al[30] described a methodology for extending the EMCM method to analytic (non-Monte Carlo) dose calculation algorithms, and detailed fundamental and dosimetric differences between EMCM and direct dose mapping for dose accumulation in the context of 4D planning for 10 lung cancer patients. While the mean differences in deformable accumulated doses to the planning target volume (PTV) between EMCM and direct dose mapping were generally small (within 1%-2% of each other), local differences in the PTV minimum doses were sometimes much larger (up to 11%). These largest dose differences were observed in regions with sharp mass density variations and/or high dose gradients.[30] Ziegenhein et al[31] developed a fast, on-line implementation of the EMCM approach and achieved significant improvement in computation speed through use of single-core optimization, parallelization for multiple cores and vectorization.

Deformable Dose Mapping: Uncertainty Estimation

With the realization that errors and uncertainties in deformable image registration translate to the mapped and accumulated dose distributions, many investigators have sought out approaches to estimate the impact of these uncertainties in the mapped dose distributions.[23,24,32-44] Here, we present some examples to illustrate the variety of techniques proposed.

Rosu et al[23] investigated dose grid resolution effects and found that, in general, differences between dose grid interpolation schemes occur in high dose gradient regions and are unlikely to result in clinically significant differences for volume-effect organs (eg, lung tissue), but should be viewed more carefully for serial organs (eg, spinal cord) with consideration of tumor location, magnitude of deformation, motion, and tissue heterogeneity.[23]

Hub et al[32] evaluated dose mapping and registration metric sensitivities to variations of the parameters of a b-spline-based deformable algorithm. Their approach was able to distinguish between areas with larger vs smaller dose mapping uncertainties, though it was not designed to estimate absolute dose mapping uncertainties.

Similar research was performed by Yibing et al,[45] who evaluated uncertainty in dose mapping after performing deformable registration between planning CT and daily CT images 132 times using a range of parameter settings for the registration algorithm for patients with liver cancer. Based on selection of "realistic" registrations, they showed that voxel position uncertainties were 5.6 ± 3.3 mm (at the 99th percentile). The subsequent variation in accumulated maximum dose in hollow OARs (difference between 1st and 99th percentile) was up to 3.3 Gy.[45]

Murphy et al[33] examined DVF errors due to choice of the selected region-of-interest and created associated DVF maps, which were analyzed using principal components analysis. They showed their error sampling method to produce synthetic DVF uncertainty maps that were statistically equivalent to observed error maps.[33]

Salguero et al[36] pointed out that the intrinsic lack of inverse consistency during deformable registration can be used as a measure from which to estimate the DVF uncertainty, and subsequently the dose mapping uncertainty. They showed for a 4D lung plan that the standard deviation of inconsistency vectors (induced by mapping 62.6 Gy) was up to 9.2 mm (with mean of 1.3 mm) translating to a maximum dose uncertainty of 21.8 Gy. Uncertainty, comparison between deformable dose algorithms with and without inverse consistency constraints for head/neck cancer patients was performed by Veiga et al.[46]

Bender et al[38] sought to reduce inverse consistency and transitivity errors in deformable registration using a constrained, diffeomorphic (topology preserving) registration algorithm, which lead to consistent dose accumulation results regardless of the deformable mapping pathway (source-to-target, or target-to-source). Yan et al[39] defined a dose mapping error based on the assumption that the average dose accumulated in a finite volume should be unchanged when tissue deformation between the anatomic instances is mass conserving, such as in the case of respiratory-induced motion of normal lung tissue. Risholm et al[34] and Tilly et al[37] modeled deformable registration uncertainties as multivariate Gaussian distributions to estimate the uncertainty in accumulated dose distributions, for example head/neck and prostate cases, respectively.

Tilly et al[37] observed that the planning parameter most sensitive to the DIR uncertainty was the target dose coverage, D95. They noted that a registration mean absolute ≤0.20 cm was necessary to obtain uncertainty in D95 of within 3% for intermediate-sized penumbras. They also pointed out that use of larger planning margins (clinical target volume (CTV)-to-PTV) relaxed registration uncertainty requirements albeit at the cost of increased dose to OARs.[37] Zhong et al[47,48] applied the principle of conservation of energy to evaluate deformable dose mapping operations performed with different algorithms under conditions of tumor regression and tumor mass loss in the context of adaptive radiotherapy (ART) for patients with non−small cell lung cancer.

Biomechanical models, previously applied to characterize normal organ structure,[49] have also been developed for the purposes of deformable image registration and dose accumulation.[21,50-53] Biomechanical models characterize organs by discretizing the tissue into many small elements, which are assigned linear-elastic properties representing the tissue of interest. Although these models are also subject to uncertainties pertaining to applied boundary conditions,[54] assignment of accurate material properties,[55,56] etc. carefully validated biomechanical models can serve as accuracy benchmarking tools for validation of intensity-based deformable registration algorithms.[38,51,52,57,58] A disadvantage of biomechanical models is that they are computationally burdensome, however, accurate hybrid approaches, in which intensity-based (eg, B-spline) algorithms are combined with finite element models are significantly more efficient.[40,59,60] Biomechanical models have also been used to estimate uncertainties in the dose accumulation process. In one such example, Brock et al[61] evaluated dose accumulation using a biomechanical model to warp dose in the context of 4D planning for liver cancers, and compared the mapped doses between 2 models, one which incorporated liver deformation and one which was based purely on a static (rigid) mapping. They showed average changes in prescribed doses between static and deformed doses for simulated tumors ranging from 2.1 Gy to 27.0 Gy depending on the location of the tumor, and respective changes of 0.4 Gy (−4.1 to 1.7 Gy) for the patient's actual tumor.[61]

Phantoms designed to measure dose under conditions where tissues deform theoretically offer the most objective assessment of the accuracy of the deformable dose accumulation algorithm. Investigators have fabricated phantoms to mimic tissue deformation and in some instances have included detectors to measure radiation in the deforming tissue.[62-68] In practice, it is quite difficult to design phantoms that can mimic tissue deformation in a clinically realistic manner. Moreover, the types of dosimeters used in these phantoms are often limited to point-based measurements, which restrict evaluation of the delivered dose in a plane or volume. Gel dosimeters under conditions of deformation offer a potential solution to the lack of volume-based measurements, with other detectors.[66] Gels enable measurement of voxel-based deformable dose estimates under conditions where the intensity distribution is uniform (considering that gels are typically homogeneous in texture), which is beneficial for validating intensity-based algorithms often suffering from inaccuracies in regions with uniform image intensity.[51,52]

As demonstrated in the above (and other) studies, lack of ground truth often requires validation of mapped dose using known DVFs in physical or simulated phantoms. Methods for validating deformable dose mapping in the clinically realistic setting are necessary, and are likely to lead to faster uptake of the deformable dose mapping process in the routine clinical setting. Research on this topic is highly encouraged.

Application of Deformable Dose Accumulation to ART

The increased utilization of imaging in radiation oncology has accelerated interest in the assessment of anatomical changes arising in target and healthy organs during the course of radiation therapy. In particular, the development of volumetric imaging in the treatment room, cone-beam CT,[69] has significantly enabled the application of ART[70] in which volumetric imaging information is used to update the patient model, and subsequently used to compute the "dose-of-the-day" for comparison with original treatment plan. An important step prior to comparison of daily or mid-treatment doses involves deformable dose mapping and accumulation from dose-of-the-day on a respective daily or mid-treatment dataset to the planning CT. There has been much research devoted toward understanding adaptive changes in dose for various treatment anatomies from the head/neck to the pelvis.[71-78] Much effort has been dedicated to developing tools that would allow objective, accurate, and fast evaluation of the dose-of-the day using the anatomy-of-the-day acquired from pretreatment CBCT images.

In one approach, doses are computed directly on the CBCT. The workflow involves dose calculation on each CBCT dataset, which is then mapped to the planning CT (pCT) and accumulated using the DVF generated during deformable registration of the CBCT to pCT. CBCT images, however, can be of poor quality due to artifacts and reduced contrast, particularly in situations where patient scatter is high. These issues impact on the ability to generate a reliable HU-to-electron density conversion, as required for dose calculation. Multiple approaches have been proposed to address this topic, ranging from phantom-based calibrations to individual treatment sites calibrations, using the knowledge of the image intensity levels or tissue densities, as well as density override approaches from pCT to CBCT.[79-83]

Another method for mapping doses (see Fig. 6 from Veiga et al[46]) involves the generation of a resampled or "synthetic CT" formed by deforming the pCT to the CBCT.[46,84] Post-processing techniques on the image datasets, such as histogram equalization, can be used to enhance the registration accuracy.[84,85] Dose is then computed on the synthetic CT, which potentially circumvents issues related to HU, noise, and other factors impacting accuracy of the CBCT. Another difficulty associated with dose calculations on CBCT is the limited craniocaudal length and field-of-view, which can be problematic for proper dose computation and deformable mapping for sites, such as the head and neck. Different approaches have been proposed to address the limited field-of-view problem, including extrapolation of the CBCT dataset based on deformation with the pCT.[86,87]

In addition to ART, the management of tumor and normal tissue response following radiotherapy based on follow-up CT, MRI, PET (or other image modalities) also necessitates proper deformable dose mapping approaches in order to be able to establish accurate dose-volume-effect relationships. This process is muddied by the significant changes in the tumor and normal tissue anatomy months after radiotherapy. Issues,[88-91] such as regression of the tumor, differentiation between tumor vs fibrotic changes, normal tissue density and mass changes, etc., are all highly relevant and impact on the accuracy of deformable dose accumulation, and must therefore be considered carefully.

Deformable Dose Mapping: Considerations

The concept of dose while conceptually straightforward is not without controversy. Debates on the appropriateness of deforming dose along with deformable image registration,[92] as well different approaches for accurate deformable dose accumulation have been on-going.[93-96] As discussed by Schultheiss and Tomé,[92] there are several factors influencing the accuracy of deformable dose accumulation, including issues related to image distortion, noise, artifacts, and tumor and normal tissue motion. While these errors will impact directly on the accuracy of the deformably mapped organs/contours, visual verification of these contours is at least possible to estimate the accuracy of the registration. However, with regard to dose, there are no qualitative or quantitative approaches to which to assess the deformed dose distributions. This issue is further confounded by the fact that the voxel-based mapping of deformed dose does not account for cellular spatial changes, such as regression of some types of solid tumors, as well reduction in volume of normal tumors, for example parotid glands during fractionated radiotherapy.[92] It is difficult to quantify the level of uncertainty in deformed dose distributions in light of these factors. Therefore, the question of whether or not it is better to provide an uncertain estimate of the deformed dose during ART or not to deform dose at all, is indeed of relevance.[92]

Perhaps one reasonable approach is to assess individual patient circumstances, and to exercise caution under conditions in which tumors and/or normal tissues are noted to exhibit significant changes during radiotherapy.[94,96] It is likely that current intensity-based deformable algorithms are inaccurate under such situations. In order to appreciate the limitations, one must gain understanding into the manner in which tumors regress in response to radiation. As pointed out by Schultheiss and Tomé,[92] this is not a facile problem. However, based on clinical observations,[97-99] it is possible that different models of tumor regression can provide plausible descriptions of tumor response for different treatment sites. Figures 6 and 7 provide 2 possible modes of tumor regression, as suggested previously.[71,100,101]

In the first case (Fig. 7), the tumor regresses elastically possibly without leaving behind microscopic extension, and the surrounding normal tissue moves concentrically with the tumor border. In the second case (Fig. 8), the tumor does not regress elastically, potentially leaving behind microscopic, extracapsular spread, and the normal tissue generally remains intact while the tumor boundary regresses. Lung tumors have generally exhibited dose response typical of the first case,[97,98] whereas head and

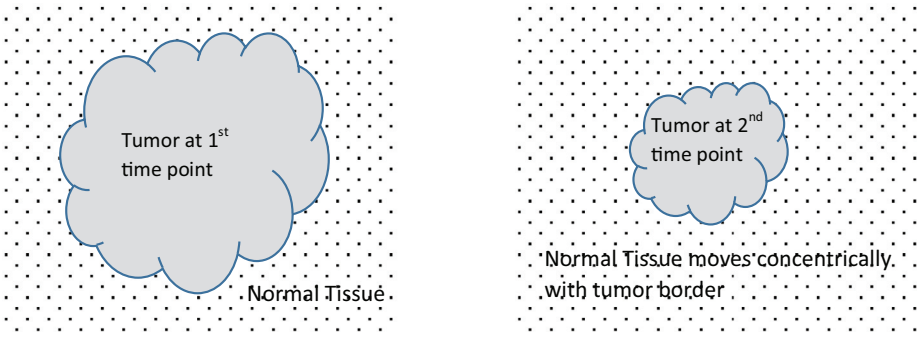

Figure 7 Left: Tumor and surrounding tissue at initial time point. Right: Tumor regressing "elastically" with normal tissue moving concentrically with tumor border.

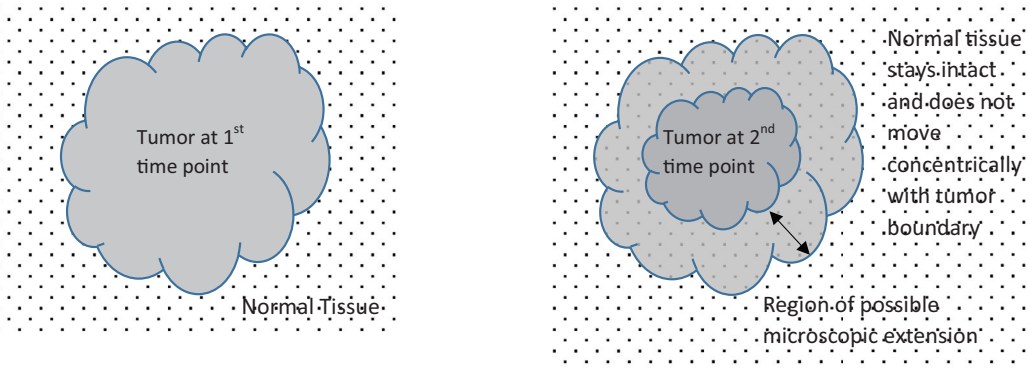

Figure 8 Left: Tumor and surrounding tissue at initial time point. Right: Tumor regressing "inelastically" with possible regions of microscopic extension. Normal tissue does not move concentrically with tumor border.

neck tumors with extracapsular extension resemble the second regression method.[99] With elastic regression, it may be reasonable to assume that adaptation of the planning margins according to the tumor boundary is safe; however, in situations where microscopic extension is present, it is likely unsafe to reduce planning margins even if the geometric tumor boundary regresses.

As demonstrated previously, the use of typical deformable algorithms to map dose from the regressed tumor in the second time point to the initial tumor mass first time point is likely to be inaccurate.[94] This is because most DIR algorithms are based on the intensity similarity of the 2 image sets being registered, and consequently the deformation maps will tend to align the border of the regressed tumor mass with that of the initial tumor. From a dose perspective, this means that regardless of the tumor mass change, the dose in the regressed tumor is forced to be the same as that in the initial mass, implying that energy has been created, thereby resulting in a physically intractable solution.[94] Intensity-based deformable algorithms map dose without consideration of the spatial regression modes of the tumor as described above.[93-95] For the case of elastic regression, it is likely that a volume-preserving or a rigid mapping of the dose in the regressed tumor to that in the original tumor will provide a better estimate of the accumulated dose. For the case where the tumor undergoes inelastic mass changes, deformable dose mapping from the regressed to the initial tumor masses will not properly account for dose to the normal tissue surrounding the regressed tumor mass, which may not move in concert with the tumor boundary.[71,94]

Another relevant consideration toward the goal of accurate dose estimation for ART is related to summation of doses for different fractionation regimens. There are 2 considerations here. First, the physical doses delivered and summed to targets and OARs will be different based on the type of registration performed to map doses, which implies that the biologically equivalent doses will be different, regardless of the type of biological model applied. Second, the biological model used for the conversion of physical to biologically equivalent dose will also have an impact on the accumulated dose. Boman et al[102] performed dose summation for clinical retreatment plans using 3 different summation methods: (1) rigid registration of planning images and direct (physical) dose summing; (2) deformable registration of planning images and direct (physical) dose summing; and (3) deformable registration of planning images biologically equivalent dose summing, applying the linear-quadratic model. They showed that differences between deformable direct, and rigid direct dose summations was in the range of −8 to 2 Gy in the maximum OAR doses (D0.1cc), with corresponding differences in the range of −14 to 5 Gy between deformable biological and rigid biological dose summations. They surmised that the differences arise from incorrect summation of doses in the rigid direct sum case (relative to deformable summation), and

from the dose per fraction effect in biological summation (relative to direct, physical dose summation).[102] With regard to the type of biological model used for the dose summation, the linear quadratic model has served as the benchmark method for estimation of biological dose especially in the context of conventional fractionation regimens (2 Gy/fraction). Modifications to the linear quadratic model for hypofractionated regimens (>10 Gy/fraction) to better fit empirical data, as well as other models have been proposed, and is the subject of ongoing investigation.[103-106]

Discussion

Deformable dose accumulation is a foundational requirement for ART. In order to accurately model dose-volume-effect relationships over the course of fractionated radiotherapy in the context of ART, or for response assessment following radiotherapy, it is necessary to accumulate doses to tumors and normal tissues[107] in the face of tumor and/or normal tissue changes. Deformable dose algorithms are limited in complexity with regard to cellular changes that occur in tumors and normal organs during fractionated radiotherapy, and consequently accurate voxel-based dose mapping is especially challenging under circumstances where mass is altered. Based on clinical observations of different treatment sites, it might be possible to construct approximate models of tumor regression patterns, which can in turn be used to intelligently constrain the deformable registration algorithms, thereby leading to better estimates of the deformed dose. As a field, it is important that we understand the limitations of the readily available tools we have at our disposal for deformable dose accumulation, and importantly that we exercise caution in applying these tools without careful consideration of the possible uncertainties. In this regard, it is imperative that the clinical team evaluate the adaptive changes for each individual patient – indeed, there may be some circumstances where tumor and/or normal tissue mass changes are deemed unreasonable, in which case restraint on the use of deformable dose accumulation may be warranted.

Ultimately, the impact on patients of deformable dose accumulation for ART is of central concern. It would behoove us to develop consistent methodologies to accurately deform dose, such that clinical outcomes can be correlated with the deformed dose distributions in a dependable manner. Clinical trials are necessary to evaluate the possible clinical benefit of ART.[108-110] The results of our clinical experiences are likely to produce more compelling results (specifically deformable dose-volume-effect relationships) if consistent deformable registration and dose mapping methodologies are applied uniformly for different treatment sites and regression models.

Finally, the clinical resources required for deformable dose accumulation for ART are not insignificant, as one needs to validate the accuracy of the deformable image registration algorithms and the resulting accumulated dose distributions prior to clinical application.[78,96] This represents a paradigm shift from our conventional treatment approach, and may well require additional staffing resources for successful implementation. The development of automated tools to enable high-quality ART is likely to lead to efficiency gains, in addition to fostering clinical uptake.

References

1. Chen GT, Sharp GC, Mori S: A review of image-guided radiotherapy. Radiol Phys Technol 2:1-12, 2009
2. Jaffray DA, Chung C, Coolens C, et al: Quantitative imaging in radiation oncology: An emerging science and clinical service. Semin Radiat Oncol 25:292-304, 2015
3. van Herk M: Different styles of image-guided radiotherapy. Semin Radiat Oncol 17:258-267, 2007
4. Viergever MA, Maintz JBA, Klein S, et al: A survey of medical image registration – under review. Med Image Anal 33:140-144, 2016
5. Brock KK: Image Processing in Radiation Therapy. In: Brock KK, ed. (ed 1): Boca Raton, FL: CRC Press, Taylor & Francis Group; 2013:ix-xiii
6. Brock KK, Mutic S, McNutt TR, et al: Use of image registration and fusion algorithms and techniques in radiotherapy: Report of the AAPM Radiation Therapy Committee Task Group No. 132. Med Phys 44:e43-e76, 2017
7. Crum WR, Hartkens T, Hill DL: Non-rigid image registration: Theory and practice. Br J Radiol 77(Spec No 2):S140-S153, 2004
8. Kessler ML: Image registration and data fusion in radiation therapy. Br J Radiol 79(Spec No 1):S99-108, 2006
9. Maintz JBA, Viergever MA: A survey of medical image registration. Med Image Anal 2:1-36, 1998
10. Oliveira FPM, Tavares JMRS: Medical image registration: A review. Comput Methods Biomech Biomed Eng 17:73-93, 2014
11. Sotiras A, Christos D, Paragios N: Deformable medical image registration: A survey, Research Report RR-7919, <hal-00684715v00684713>; 2012.
12. Oh S, Kim S: Deformable image registration in radiation therapy. Radiat Oncol J 35:101-111, 2017
13. Hill DL, Batchelor PG, Holden M, et al: Medical image registration. Phys Med Biol 46:R1-45, 2001
14. Paganelli C, Meschini G, Molinelli S, et al: Patient-specific validation of deformable image registration in radiation therapy: Overview and caveats. Med Phys 45:e908-e922, 2018
15. Christensen GE, Rabbitt RD, Miller MI: 3D brain mapping using a deformable neuroanatomy. Phys Med Biol 39:609, 1994
16. Christensen GE, Song JH, Lu W, et al: Tracking lung tissue motion and expansion/compression with inverse consistent image registration and spirometry. Med Phys 34(6 Part1):2155-2163, 2007
17. Guetter C, Xue H, Chefd'hotel C, et al: Efficient symmetric and inverse-consistent deformable registration through interleaved optimization. In: 2011 IEEE International Symposium on Biomedical Imaging: From Nano to Macro; 2011. p. 590-593
18. Xuejun G, Hubert P, Yun L, et al: Implementation and evaluation of various demons deformable image registration algorithms on a GPU. Phys Med Biol 55:207, 2010
19. Yang D, Brame S, El Naqa I, et al: Technical note: DIRART – A software suite for deformable image registration and adaptive radiotherapy research. Med Phys 38:67-77, 2011
20. Yang D, Li H, Low DA, et al: A fast inverse consistent deformable image registration method based on symmetric optical flow computation. Phys Med Biol 53:6143-6165, 2008
21. Brock KK, Sharpe MB, Dawson LA, et al: Accuracy of finite element model-based multi-organ deformable image registration. Med Phys 32:1647-1659, 2005
22. Paganetti H, Jiang H, Adams JA, et al: Monte Carlo simulations with time-dependent geometries to investigate effects of organ motion with high temporal resolution. Int J Radiat Oncol Biol Phys 60:942-950, 2004
23. Rosu M, Chetty IJ, Balter JM, et al: Dose reconstruction in deforming lung anatomy: Dose grid size effects and clinical implications. Med Phys 32:2487-2495, 2005
24. Rosu M, Hugo GD: Advances in 4D radiation therapy for managing respiration: Part II – 4D treatment planning. Z Med Phys 22:272-280, 2012

25. Schaly B, Kempe JA, Bauman GS, et al: Tracking the dose distribution in radiation therapy by accounting for variable anatomy. Phys Med Biol 49:791-805, 2004
26. Heath E, Seuntjens J: A direct voxel tracking method for four-dimensional Monte Carlo dose calculations in deforming anatomy. Med Phys 33:434-445, 2006
27. Heath E, Tessier F, Kawrakow I: Investigation of voxel warping and energy mapping approaches for fast 4D Monte Carlo dose calculations in deformed geometries using VMC++. Phys Med Biol 56:5187-5202, 2011
28. Siebers JV, Zhong H: An energy transfer method for 4D Monte Carlo dose calculation. Med Phys 35:4096-4105, 2008
29. Zhong H, Siebers JV: Monte Carlo dose mapping on deforming anatomy. Phys Med Biol 54:5815-5830, 2009
30. Li HS, Zhong H, Kim J, et al: Direct dose mapping versus energy/mass transfer mapping for 4D dose accumulation: fundamental differences and dosimetric consequences. Phys Med Biol 59:173-188, 2014
31. Ziegenhein P, Kamerling CP, Fast MF, et al: Real-time energy/mass transfer mapping for online 4D dose reconstruction. Sci Rep 8:3662, 2018
32. Hub M, Thieke C, Kessler ML, et al: A stochastic approach to estimate the uncertainty of dose mapping caused by uncertainties in b-spline registration. Med Phys 39:2186-2192, 2012
33. Murphy MJ, Salguero FJ, Siebers JV, et al: A method to estimate the effect of deformable image registration uncertainties on daily dose mapping. Med Phys 39:573-580, 2012
34. Risholm P, Balter J, Wells WM: Estimation of delivered dose in radiotherapy: The influence of registration uncertainty. Med Image Comput Comput Assist Interv 14(Pt 1):548-555, 2011
35. Saleh-Sayah NK, Weiss E, Salguero FJ, et al: A distance to dose difference tool for estimating the required spatial accuracy of a displacement vector field. Med Phys 38:2318-2323, 2011
36. Salguero FJ, Saleh-Sayah NK, Yan C, et al: Estimation of three-dimensional intrinsic dosimetric uncertainties resulting from using deformable image registration for dose mapping. Med Phys 38:343-353, 2011
37. Tilly D, Tilly N, Ahnesjo A: Dose mapping sensitivity to deformable registration uncertainties in fractionated radiotherapy — Applied to prostate proton treatments. BMC Med Phys 13:2, 2013
38. Bender ET, Hardcastle N, Tome WA: On the dosimetric effect and reduction of inverse consistency and transitivity errors in deformable image registration for dose accumulation. Med Phys 39:272-280, 2012
39. Yan C, Hugo G, Salguero FJ, et al: A method to evaluate dose errors introduced by dose mapping processes for mass conserving deformations. Med Phys 39:2119-2128, 2012
40. Samavati N, Velec M, Brock KK: Effect of deformable registration uncertainty on lung SBRT dose accumulation. Med Phys 43:233, 2016
41. Schreibmann E, Pantalone P, Waller A, et al: A measure to evaluate deformable registration fields in clinical settings. J Appl Clin Med Phys 13:3829, 2012
42. Schreibmann E, Xing L: Image registration with auto-mapped control volumes. Med Phys 33:1165-1179, 2006
43. King M, Sensakovic WF, Maxim P, et al: Line-enhanced deformable registration of pulmonary computed tomography images before and after radiation therapy with radiation-induced fibrosis. Technol Cancer Res Treat 17. 1533034617749419
44. Guy CL, Weiss E, Christensen GE, et al: CALIPER: A deformable image registration algorithm for large geometric changes during radiotherapy for locally advanced non-small cell lung cancer. Med Phys 45:2498-2508, 2018
45. Yibing W, Steven FP, Eliana Vásquez O, et al: An individualized strategy to estimate the effect of deformable registration uncertainty on accumulated dose in the upper abdomen. Phys Med Biol 63:125005
46. Veiga C, Lourenco AM, Mouinuddin S, et al: Toward adaptive radiotherapy for head and neck patients: Uncertainties in dose warping due to the choice of deformable registration algorithm. Med Phys 42:760-769, 2015
47. Zhong H, Chetty IJ: Adaptive radiotherapy for NSCLC patients: Utilizing the principle of energy conservation to evaluate dose mapping operations. Phys Med Biol 62:4333-4345, 2017
48. Zhong H, Siddiqui SM, Movsas B, et al: Evaluation of adaptive treatment planning for patients with non-small cell lung cancer. Phys Med Biol 62:4346-4360, 2017
49. Matthews FL, West JB: Finite element displacement analysis of a lung. J Biomech 5:591-600, 1972
50. Brock KK, Hollister SJ, Dawson LA, et al: Technical note: Creating a four-dimensional model of the liver using finite element analysis. Med Phys 29:1403-1405, 2002
51. Velec M, Juang T, Moseley JL, et al: Utility and validation of biomechanical deformable image registration in low-contrast images. Pract Radiat Oncol 5:e401-e408, 2015
52. Zhong H, Kim J, Li H, et al: A finite element method to correct deformable image registration errors in low-contrast regions. Phys Med Biol 57:3499-3515, 2012
53. Zhong H, Wachowiak MP, Peters TM: A real time finite element based tissue simulation method incorporating nonlinear elastic behavior. Comput Methods Biomech Biomed Eng 8:177-189, 2005
54. Samavati N, McGrath DM, Lee J, et al: SU-E-J-95: Towards optimum boundary conditions for biomechanical model based deformable registration using intensity based image matching for prostate correlative pathology. Med Phys 39:3674, 2012
55. Carter TJ, Sermesant M, Cash DM, et al: Application of soft tissue modelling to image-guided surgery. Med Eng Phys 27:893-909, 2005
56. Tanner C, Schnabel JA, Hill DL, et al: Factors influencing the accuracy of biomechanical breast models. Med Phys 33:1758-1769, 2006
57. Zhong H, Kim J, Chetty IJ: Analysis of deformable image registration accuracy using computational modeling. Med Phys 37:970-979, 2010
58. Yan D, Jaffray DA, Wong JW: A model to accumulate fractionated dose in a deforming organ. Int J Radiat Oncol Biol Phys 44:665-675, 1999
59. Sharifi H, Zhang H, Bagher-Ebadian H, et al: Utilization of a hybrid finite-element based registration method to quantify heterogeneous tumor response for adaptive treatment for lung cancer patients. Phys Med Biol 63:065017
60. Zhong H, Wen N, Gordon JJ, et al: An adaptive MR-CT registration method for MRI-guided prostate cancer radiotherapy. Phys Med Biol 60:2837-2851, 2015
61. Brock KK, McShan DL, Ten Haken RK, et al: Inclusion of organ deformation in dose calculations. Med Phys 30:290-295, 2003
62. Fusella M, Giglioli FR, Fiandra C, et al: Evaluation of dose recalculation vs dose deformation in a commercial platform for deformable image registration with a computational phantom. Med Dosim 43:82-90, 2018
63. Ger RB, Yang J, Ding Y, et al: Accuracy of deformable image registration on magnetic resonance images in digital and physical phantoms. Med Phys 44:5153-5161, 2017
64. Graves YJ, Smith AA, McIlvena D, et al: A deformable head and neck phantom with in-vivo dosimetry for adaptive radiotherapy quality assurance. Med Phys 42:1490-1497, 2015
65. Lu J, Ma Y, Chen J, et al: Assessment of anatomical and dosimetric changes by a deformable registration method during the course of intensity-modulated radiotherapy for nasopharyngeal carcinoma. J Radiat Res 55:97-104, 2014
66. Niu CJ, Foltz WD, Velec M, et al: A novel technique to enable experimental validation of deformable dose accumulation. Med Phys 39:765-776, 2012
67. Singhrao K, Kirby N, Pouliot J: A three-dimensional head-and-neck phantom for validation of multimodality deformable image registration for adaptive radiotherapy. Med Phys 41:121709
68. Zhong H, Adams J, Glide-Hurst C, et al: Development of a deformable dosimetric phantom to verify dose accumulation algorithms for adaptive radiotherapy. J Med Phys 41:106-114, 2016
69. Jaffray DA, Siewerdsen JH, Wong JW, et al: Flat-panel cone-beam computed tomography for image-guided radiation therapy. Int J Radiat Oncol Biol Phys 53:1337-1349, 2002
70. Yan D, Vicini F, Wong J, et al: Adaptive radiation therapy. Phys Med Biol 42:123-132, 1997
71. Sonke JJ, Belderbos J: Adaptive radiotherapy for lung cancer. Semin Radiat Oncol 20:94-106, 2010

72. Brock KK, Dawson LA: Adaptive management of liver cancer radiotherapy. Semin Radiat Oncol 20:107-115, 2010
73. Castadot P, Lee JA, Geets X, et al: Adaptive radiotherapy of head and neck cancer. Semin Radiat Oncol 20:84-93, 2010
74. Ghilezan M, Yan D, Martinez A: Adaptive radiation therapy for prostate cancer. Semin Radiat Oncol 20:130-137, 2010
75. Pos F, Remeijer P: Adaptive management of bladder cancer radiotherapy. Semin Radiat Oncol 20:116-120, 2010
76. Tanderup K, Georg D, Pötter R, et al: Adaptive management of cervical cancer radiotherapy. Semin Radiat Oncol 20:121-129, 2010
77. Kumarasiri A, Liu C, Siddiqui F, et al: Target and organ dose estimation from intensity modulated head and neck radiation therapy using 3 deformable image registration algorithms. Pract Radiat Oncol 5: e317-e325, 2015
78. Lim-Reinders S, Keller BM, Al-Ward S, et al: Online adaptive radiation therapy. Int J Radiat Oncol Biol Phys 99:994-1003, 2017
79. Fotina I, Hopfgartner J, Stock M, et al: Feasibility of CBCT-based dose calculation: Comparative analysis of HU adjustment techniques. Radiother Oncol 104:249-256, 2012
80. Hatton J, McCurdy B, Greer PB: Cone beam computerized tomography: The effect of calibration of the Hounsfield unit number to electron density on dose calculation accuracy for adaptive radiation therapy. Phys Med Biol 54:N329-N346, 2009
81. Kowatsch M, Winkler P, Zurl B, et al: Analysis of image quality and dose calculation accuracy in cone beam CT acquisitions with limited projection data (half scan, half fan) with regard to usability for adaptive radiation therapy treatment planning. Z Med Phys 21:11-18, 2011
82. Yang Y, Schreibmann E, Li T, et al: Evaluation of on-board kV cone beam CT (CBCT)-based dose calculation. Phys Med Biol 52:685-705, 2007
83. Yoo S, Yin FF: Dosimetric feasibility of cone-beam CT-based treatment planning compared to CT-based treatment planning. Int J Radiat Oncol Biol Phys 66:1553-1561, 2006
84. Liu C, Kim J, Kumarasiri A, et al: An automated dose tracking system for adaptive radiation therapy. Comput Methods Progr Biomed 154:1-8, 2018
85. Kim J, Yin FF, Zhao Y, et al: Effects of x-ray and CT image enhancements on the robustness and accuracy of a rigid 3D/2D image registration. Med Phys 32:866-873, 2005
86. Liu C, Kumarasiri A, Chetvertkov M, et al: Geometric uncertainty in CBCT extrapolation for head and neck adaptive radiotherapy. Med Phys 41:189, 2014
87. Zhen X, Yan H, Zhou L, et al: Deformable image registration of CT and truncated cone-beam CT for adaptive radiation therapy. Phys Med Biol 58:7979-7993, 2013
88. Bogot NR, Quint LE: Imaging of recurrent lung cancer. Cancer Imaging 4:61-67, 2004
89. Diot Q, Kavanagh B, Vinogradskiy Y, et al: Lung deformations and radiation-induced regional lung collapse in patients treated with stereotactic body radiation therapy. Med Phys 42:6477-6487, 2015
90. Kong FM, Frey KA, Quint LE, et al: A pilot study of [18F]fluorodeoxyglucose positron emission tomography scans during and after radiation-based therapy in patients with non small-cell lung cancer. J Clin Oncol 25:3116-3123, 2007
91. Vinogradskiy Y, Diot Q, Kavanagh B, et al: Spatial and dose-response analysis of fibrotic lung changes after stereotactic body radiation therapy. Med Phys 40:081712
92. Schultheiss TE, Tome WA, Orton CG: Point/counterpoint: It is not appropriate to "deform" dose along with deformable image registration in adaptive radiotherapy. Med Phys 39:6531-6533, 2012
93. Hugo GD, Dial C, Siebers JV: In regard to Zhong and Chetty. Int J Radiat Oncol Biol Phys 99:1308-1310, 2017
94. Zhong H, Chetty IJ: Caution must be exercised when performing deformable dose accumulation for tumors undergoing mass changes during fractionated radiation therapy. Int J Radiat Oncol Biol Phys 97:182-183, 2017
95. Zhong H, Chetty IJ: In reply to Hugo et al.. Int J Radiat Oncol Biol Phys 99:1310, 2017
96. Chetty IJ, Fontenot J: Adaptive radiation therapy: Off-line, on-line, and in-line? Int J Radiat Oncol Biol Phys 99:689-691, 2017
97. Guckenberger M, Richter A, Wilbert J, et al: Adaptive radiotherapy for locally advanced non-small-cell lung cancer does not underdose the microscopic disease and has the potential to increase tumor control. Int J Radiat Oncol Biol Phys 81:e275-e282, 2011
98. Kong FM, Ten Haken RK, Schipper M, et al: Effect of midtreatment PET/CT-adapted radiation therapy with concurrent chemotherapy in patients with locally advanced non-small-cell lung cancer: A phase 2 clinical trial. JAMA Oncol 3:1358-1365, 2017
99. Mermod M, Tolstonog G, Simon C, et al: Extracapsular spread in head and neck squamous cell carcinoma: A systematic review and meta-analysis. Oral Oncol 62:60-71, 2016
100. Hugo GD, Cao K, Guy C, et al: Measurement of local deformation due to lung tumor response to radiation therapy. In: The Fifth International Workshop on Pulmonary Image Analysis; 2013. p. Nagoya, Japan97-108
101. Zhong H, Kim J, Gordon JJ, et al: World congress on medical physics and biomedical engineering. In: Jaffray D, ed. IFMBE Proceedings, Springer, Cham Toronto, Canada; 2015
102. Boman E, Kapanen M, Pickup L, et al: Importance of deformable image registration and biological dose summation in planning of radiotherapy retreatments. Med Dosim 42:296-303, 2017
103. Astrahan M: Some implications of linear-quadratic-linear radiation dose-response with regard to hypofractionation. Med Phys 35:4161-4172, 2008
104. Brown JM, Carlson DJ, Brenner DJ: The tumor radiobiology of SRS and SBRT: are more than the 5 Rs involved? Int J Radiat Oncol Biol Phys 88 (2):254-262, 2014
105. Guerrero M, Li XA: Extending the linear-quadratic model for large fraction doses pertinent to stereotactic radiotherapy. Phys Med Biol 49:4825-4835, 2004
106. Park C, Papiez L, Zhang S, et al: Universal survival curve and single fraction equivalent dose: Useful tools in understanding potency of ablative radiotherapy. Int J Radiat Oncol Biol Phys 70:847-852, 2008
107. Jaffray DA, Lindsay PE, Brock KK, et al: Accurate accumulation of dose for improved understanding of radiation effects in normal tissue. Int J Radiat Oncol Biol Phys 76(suppl 3):S135-S139, 2010
108. Guckenberger M, Wilbert J, Richter A, et al: Potential of adaptive radiotherapy to escalate the radiation dose in combined radiochemotherapy for locally advanced non-small cell lung cancer. Int J Radiat Oncol Biol Phys 79:901-908, 2011
109. Schwartz DL: Current progress in adaptive radiation therapy for head and neck cancer. Curr Oncol Rep 14:139-147, 2012
110. Schwartz DL, Garden AS, Shah SJ, et al: Adaptive radiotherapy for head and neck cancer—dosimetric results from a prospective clinical trial. Radiother Oncol 106:80-84, 2013